# Electrical and Optical Simulation of Tris (8-hydroxyquinoline) Aluminium-Based Microcavity Organic Light Emitting Diode (MOLED)

J. Chan*, A. D. Rakić*, Y. T. Yeow* and A. B. Djurišić†
* School of Information Technology and Electrical Engineering,
The University of Queensland, Brisbane Qld 4072, Australia
Email: chan@itee.uq.edu.au
† Department of Physics, University of Hong Kong,
Pokfulam Road, Hong Kong

***Abstract*— A detailed examination of the emitted radiation spectrum from tris(8-hydroxyquinoline) aluminum (Alq) based OLEDs on optical and electrical models have been presented. The OLED structure is examined as a function of choice of anode material and position of the NPB/Alq interface. The simulation results have been compared to those obtained from experiments, showing good agreement in both electrical and optical characteristics. The enhancement in light emission by aligning antinode of the stand wave pattern with effective carrier recombination region has been observed.**

***Keywords-organic light emitting diode (OLED); emission layer position; recombination rate***

## I. INTRODUCTION

OLED has emerged as a potential candidate for application in display devices due to its prominent advantages in size, brightness and wide viewing angle [1-2]. In order to further improve and optimise this device for use in practical applications, device modeling of OLED characteristics is required to better understand the physical processes affecting the device performance. Continuing from our previous work, where detailed analysis of the optical radiation spectrum from microcavity-based OLED have been presented, the carrier transport analysis is included in this work to provide further insight into both optical and electrical behaviors of double layer OLED device [3].

Electrons and holes are injected into organic layers from cathode and anode respectively, transported across organic layers and then recombined to form excitons. The excitons diffuse prior to undergoing radiative or non-radiative decay. As the optical thickness of the organic layers is of the order of a wavelength, standing wave pattern is observed. When the recombination zone is aligned with the anti-nodal region of the standing wave, enhancement in light output can be observed [4-5]. Optimum recombination rate is obtained when balanced electron and hole injection and transport are achieved in the recombination region [6]. Furthermore, barrier to carrier injection and band offset in the organic layers are the dominant parameters that affect carrier transport behavior of the device [7]. To investigate the effects of those parameters, it is necessary to combine electrical and optical models together to examine the recombination mechanism in the OLED device so as to determine the most critical parameter associated with light generation.

In this work, we simulate electrical carrier transport characteristics (electric field, carrier density and recombination region thickness) and optical properties (field distribution and emitted radiation spectrum) of a microcavity device consisting of two organic layers with varying thicknesses of N,N′-di(naphthalene-1-yl)-N,N′-diphenylbenzidine (NPB, hole transport layer) and tris(8-hydroxyquinoline) aluminium (Alq, emitting layer). These organic layers are sandwiched between a silver (70nm) cathode and either silver or copper anode to provide different injection barrier for holes. Quartz with 1 mm thickness was used as substrate. The model fully takes into account the optical dispersion in all the layers in the structure. The organic layer thickness values were chosen so that the position of the emission region was not too close to the metal cathode to avoid unrealistic model predictions since the model does not take into account exciton quenching due to defect states introduced during metal deposition. The calculated optical emission spectrum has been compared with the experimental results for Quartz/Cu/NPB/Alq/Ag device. The paper first describes the optical and electrical simulation models used including the simulation parameters and simulated experimental conditions. The outcome of simulation is then compared with the existing experimental data.

## II. DESCRIPTION OF THE MODEL

### A. Electrical model

Inside the organic semiconductor the electrical transport is modeled by the one-dimensional time-independent drift-diffusion model [7-9], which solves for a self-consistent solution of electron density, $n$, hole density, $p$ and potential $\psi$ (using the semiconductor solver Atlas [10]). The model includes:

*1) The continuity equation for n (electrons) and p (holes)*

$$\frac{d}{dx}(-\mu_n n\frac{d\psi}{dx}+D_n\frac{dn}{dx})=R \quad (1)$$
$$\frac{d}{dx}(\mu_p p\frac{d\psi}{dx}+D_p\frac{dp}{dx})=R$$

where $\mu_n$ and $\mu_p$ are the electron and hole mobilities and $D_n$ and $D_p$ are diffusion constants and $R$ is the recombination rate. The $\mu$ and $D$ are related by the well known Einstein relation. The carrier mobilities are modeled by the field-dependent form:

$$\mu_n(E)=\mu_{n0}\exp\left[\sqrt{\frac{E}{E_0}}\right] \quad (2)$$
$$\mu_p(E)=\mu_{p0}\exp\left[\sqrt{\frac{E}{E_0}}\right]$$

with $\mu_{n0}$ and $\mu_{p0}$ are the zero field mobilities, $E$ is the electric field and $E_0$ is the constant known as characteristic field. The recombination rate is taken to be optical only and modeled by the Langevin recombination coefficient $\gamma$ [7-8]:

$$R_{opt}=\gamma(pn-n_i^2) \quad (3)$$
$$\gamma=\frac{4\pi e\mu_R}{\varepsilon\varepsilon_0}$$

where $n_i$ is the intrinsic concentration and $\mu_R$ is effective recombination mobility, taken to be the larger of the electron and hole nobilities in the material, $\varepsilon\varepsilon_0$ is the permittivity of the material. The effect of traps in the organic layers is not included in the current electrical model as the literature indicates the inclusion of traps has no significant effect on the simulation results obtained [7].

*2) Poisson's equation*

$$\frac{d^2\psi}{dx^2}=-\frac{e}{\varepsilon\varepsilon_0}[p(x)-n(x)+N_D-N_A] \quad (4)$$

where $N_D$ and $N_A$ are the ionized donor and acceptor dopant concentrations.

These equations are solved for the p-n junction structure using Schottky contact boundary conditions between a metal (which also serves as the reflecting surface for optical modeling) and the organic layer at the anode and the cathode. The barrier heights governing carrier injections are: $\phi_{bn}$ for electrons and $\phi_{bp}$ for holes and are related to the metal work function $\phi_m$ of the electrodes and the electron affinity of the organic material $\chi_c$:

$$\phi_{bn}=(\phi_m-\chi_c) \quad (5)$$
$$\phi_{bp}=E_g-\phi_{bn}=E_g-(\phi_m-\chi_c)$$

The continuity equations and the Poisson equation are solved to obtain the carrier concentrations, electric field distributions and recombination rate. The thickness of recombination region can be determined from the recombination rate, which can be used to estimate the width of emission region (taking into account of exciton diffusion) to be included into the optical model.

*B. Optical model*

The devices with structure Quartz/Bottom-Mirror/ NPB/Alq/Ag were investigated for different combination of NPB/Alq thickness (153 nm/51 nm and 51 nm/153 nm) and for two different bottom mirror materials : Cu (25 nm) and Ag (80 nm). $R_{top}$ *and* $R_{bot}$ are reflectances of the top and the bottom mirrors of the device and were modelled using a transfer matrix method [11-13]. The calculated results were corrected for the incoherent reflection from the backside of a quartz substrate [14-16]. The refractive indices for all the thin film layers in the structure were determined by spectroscopic ellipsometry. For the quartz substrate, the refractive index was described by a Cauchy equation fit of the data tabulated in [17].

The emission spectra $I_{cav}$ were modeled using the following equation [18-19]:

$$I_{cav}(\lambda)=\frac{\frac{1-R_{bot}}{i}\sum_i\left[1+R_{top}+2\sqrt{R_{top}}\cos\left(\frac{4\pi z_i}{\lambda}-\varphi_{top}\right)\right]}{1+R_{bot}R_{top}-2\sqrt{R_{bot}R_{top}}\cos\left(\frac{4\pi L}{\lambda}-\varphi_{top}-\varphi_{bot}\right)}I_{nc}(\lambda) \quad (6)$$

where $L$ is the optical thickness of the cavity, and $\psi_{top}$ and $\psi_{bot}$ are the phase shift upon reflection and reflectivity of top and bottom mirrors respectively, $z_i$ is the optical distance of the emitting dipoles from the metal mirrors, $I_{nc}$ is the free space emission of Alq (determined from the photoluminescence measurements on the Alq film), and the summation over $i$ is performed with 1 nm step depending on the emission region thickness which is estimated based on the recombination region thickness obtained from electrical simulation taking into account of exciton diffusion length. Published studies suggest that the emission regions are usually within 10-20 nm from the HTL/$Alq_3$ interface [20].

*C. Parameters used in simulation models*

The material parameters used for modelling of carrier transport are obtained from literature [7-9]. The devices were simulated with forward bias of 5 volts. The mobility of majority carriers in the organic materials has been set to be two orders of magnitude higher than its minority carriers. Therefore NPB and Alq are assumed to act as hole transport layer (HTL) and emission (EML) layer respectively. Where the simulation model requires a large number of material parameters only a few critical parameters including barrier heights to carrier injection, bandgaps of the organic materials and carrier concentrations have marked effects on the simulated result [7].

| **Parameters** | **NPB** | **Alq** |
|---|---|---|
| Relative Permittivity | 3.0 | 3.0 |
| $\mu_{no}$ ($cm^2$/Vs) | $6.1\bullet10^{-6}$ | $1.9\bullet10^{-6}$ |
| $\mu_{po}$ ($cm^2$/Vs) | $6.1\bullet10^{-4}$ | $1.9\bullet10^{-8}$ |
| $E_0$ (V/cm) | $4.44\bullet10^{5}$ | $7.1\bullet10^{4}$ |
| Nc($cm^{-3}$) | $1\bullet10^{21}$ | $1\bullet10^{21}$ |
| Nv($cm^{-3}$) | $1\bullet10^{21}$ | $1\bullet10^{21}$ |
| $N_A$($cm^{-3}$) | $1\bullet10^{9}$ | -- |
| $N_D$($cm^{-3}$) | -- | $1\bullet10^{9}$ |
| $E_g$ (eV) | 3.0 | 2.7 |
| $\chi_c$ (eV) | 2.4 | 3.0 |
| **Parameters** | **Cu** | **Ag** |
| $\phi_m$ (eV) | 4.65 | 4.26 |

**Table 1 Electrical simulation parameters**

## III. RESULTS AND DISCUSSION

Firstly, general electrical properties of OLED structure were investigated. The electric field and carrier density of a device with 153 nm NPB (p-side) and 51nm Alq (n-side) sandwiched between Cu (25 nm) anode and Ag (70 nm) cathode was simulated as shown in fig. 1. When a forward bias voltage of 5 V was applied, holes are injected from anode into NPB layer and accumulated near the NPB/Alq interface due to offsets in the HOMO bands. Alq layer acted as a hole blocking layer in this case. On the other hand, amount of electrons injected into Alq layer from cathode is negligible due to large barrier offset $\phi_{bn}$ (1.2 eV). Accumulation of holes in the NPB/Alq interface caused electric field in Alq region to be higher than that of NPB layer according to Poisson's equation.

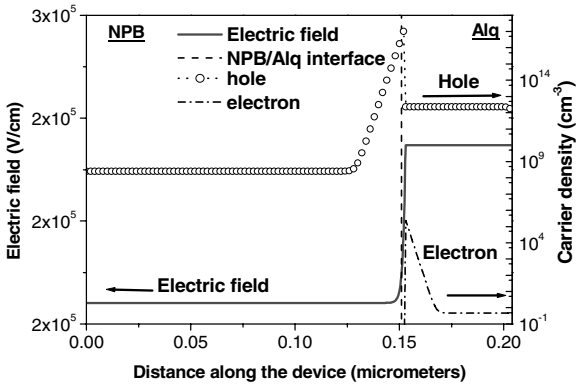


**Figure 1 Simulated electric field and carrier density of 51/153 device across the organic layers.**

Fig. 2a shows the simulated carrier recombination rate in the same device. It is clearly observed that majority of the recombination occurred within 5 nm from the NPB/Alq interface in the Alq layer. The result corresponds to Tang's finding which reported that in an Alq-based bi-layer structure, recombination zone generally occurs within 5nm from the HTL/EML interface and emission zone usually extends to 20nm due to exciton diffusion [21]. The luminance spectrum (Fig. 2b) was simulated with the emission layer thickness of 20 nm based on the recombination region thickness (5nm) obtained from the electrical simulation

The effects on the carrier transport in devices using different anode material were investigated. Device with 51 nm NPB (p-side) and 153 nm Alq (n-side) sandwiched between Ag (80 nm) anode and Ag (70 nm) cathode was simulated. The device is exactly the same as the previous one but with anode replaced with an Ag metal. The replacement increased the hole injection barrier from 0.75 to 1.14 eV and it has significantly reduced the amount of holes injected into the NPB layer, the barrier offset in the NPB/Alq interface caused holes to pile up as before. This decreased the recombination rate by two orders of magnitude compared to the previous device. The effect on the lowered recombination rate also reflected on the electro-luminance (EL). The EL of device with Ag anode is significantly lowered when compared to device with Cu anode. On the other hand, if the electron injection barrier is further increased, negligible electron will be injected into the Alq layer, thus leads to negligible recombination rate. Therefore, in order to obtained better recombination efficiency, balance injection of carriers into the emission region is essential.

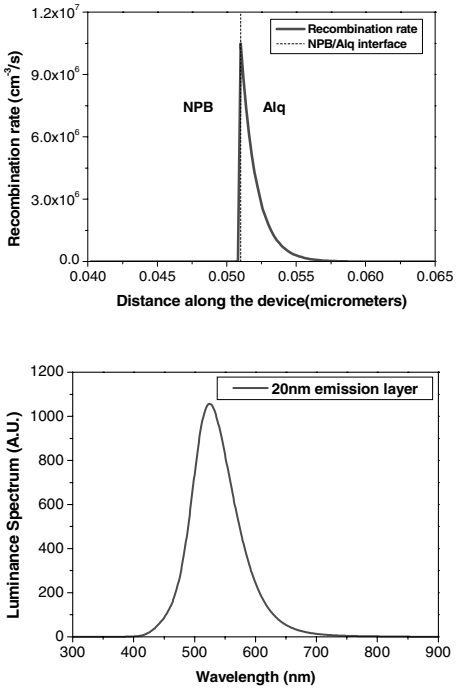


**Figure 2a Simulated carrier recombination rate of 51/153 device across the organic layers (top) Figure 2b Simulated luminance spectrum of the device one with emission layer thickness of 20nm (bottom).**

The effects of devices with different position of the NPB/Alq interface were examined. The devices have common Cu (25nm) anode and Ag (70nm) cathode, but one with 51 nm NPB and 153 nm Alq (referred as 51/153) and the other with 153 nm NPB and 51 nm Alq (referred as 153/51). Fig. 3 shows the simulated optical field intensity in these two devices. It is well known that the strongest EL enhancement is obtained when the emission layer is aligned with the position of the antinode of the cavity [22]. In 153/51 device, the peak of the field coincides with the peak of the recombination region in the vicinity of the NPB/Alq interface. On the other hand, the emission region of 51/153 device is not aligned with antinode of the optical field; in fact the emission region is positioned near the node of the optical field. This phenomenon has major effect on the EL intensity obtained (as shown in Fig. 4) for the two structures with 20 nm emission layer thickness. It is obvious that the EL intensity of 153/51 device is much greater than that of 51/153, due to coincidence of optical field antinode and emission layer which enhances the overall light output. Fig. 4 also shows the comparison between the simulated and experimental electroluminance spectra of both devices, it can be observed that the main features of the spectra agree reasonably well.

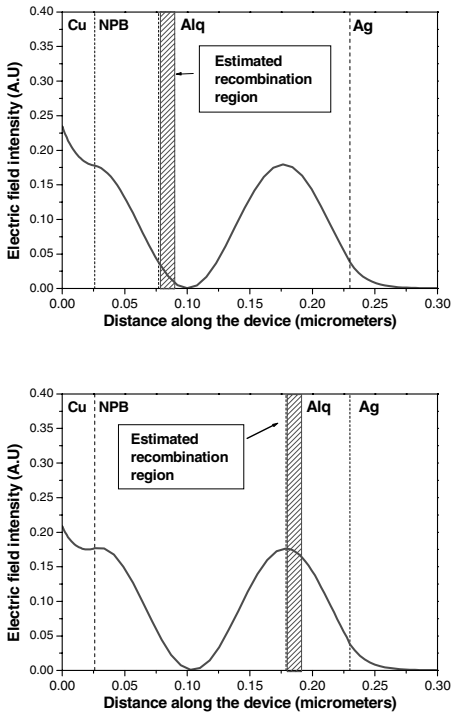


**Figure 3 simulated optical field intensity of device one with different NPB/Alq thickness of 51/153 (top) and 153/51 (bottom) respectively.**

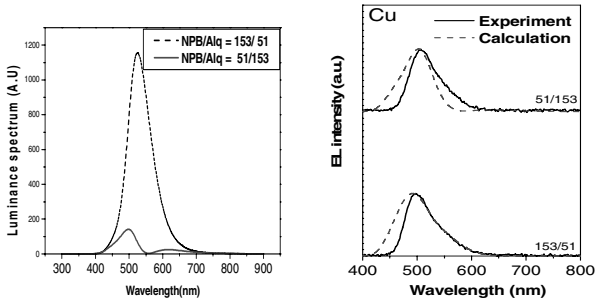


**Figure 4 Simulated Luminance spectrum for devices with 20nm of emission layer thickness (left) and comparison between the simulated and experimental electroluminance spectra of both devices (Right).**

## CONCLUSION

We have simulated both electrical and optical behavior of bilayer OLEDs by use of numerical and analytical models. The recombination width obtained from the electrical model was found to be within 5nm from NPB/Alq interface in the Alq region, which agrees with the experimental value. The calculated recombination region width was used to determine the emission layer thickness to be used in the optical simulation. In order to achieve better recombination efficiency, balanced carrier transport to the emissive layer is essential. By simulating the device with different choice of anode material, we have observed that injection barrier for electrons and holes is the major parameter that affects the carrier transport in the device. By aligning the position of the antinode of optical field intensity within the device with the electrical recombination region, enhancement in the overall light output of the device was achieved. Good agreement between the simulated and experimental electro-luminance spectra was observed.

## REFERENCES


[1] W. Brütting, S. Berleb, and A. G. Muckl, "Device physics of organic light-emitting diodes based on molecular materials", Organic Electronics **2**, pp. 1-36, March 2001.

[2] L. S. Hung and C. H. Chen, "Recent progress of molecular organic electroluminescent materials and devices", Mat. Sci. Eng. R **39**, pp. 143-202, Dec. 2002.

[3] J.Chan, A. D. Rakic, C. Y. Kwong, A. B. Djurišić, M. L. Majewski and W. K. Chan, "Optimization of organic light emitting diode structures" Proc. SPIE. 5277, pp. 311-319, 2004.

[4] S. K. So, W. K. Choi, L. M. Leung, and K. Neyts, "Interference effects in bilayer organic light-emitting diodes", Appl. Phys. Lett. **74**, pp. 1939-1941, Apr. 1999.

[5] S Dirr, A. Bohler ,S. Wiese,H. Johannes and W. Kowalsky, "Organic Light Emitting Diodes with Reduced Spectral and Spacial Halfwidth", Jpn. J. Appl. Phys. 37, pp. 1457-1461, 1998.

[6] A. B. Walker, A. Kambili and S. J. Martin, "Electrical Transport Modelling in Organic Electroluminescent Devices", J. Phys.: Condens. Matter. 14, pp. 9825-9876, 2002.

[7] S. J. Martin, G. L. B. Verschoor, M. A. Webster and A. B. Walker," The Internal Electric Field Distribution in Bilayer Organic Light Emitting Diodes", Org. elec. 3, pp. 129-141, 2002.

[8] M. A. Webster, J. Auld, S. J. Martin and A. B. Walker, "Simulation of the External Quantum Efficiency for Bilayer Organic Light Emitting Device", Proc. SPIE. 5214(1), pp 300-309, 2004.

[9] C. Blades and A. Walker, "Simulation of Organic Light-Emitting Diode", Synth. Met. 111-112, pp. 335, 2000.

[10] Silvaco, ATLAS user"s manual, Silavaco, Santa Clara, CA.

[11] R. F. Potter, in *Handbook of Optical Constants of Solids I*, edited by E. D. Palik (Academic Press Inc., San Diego, 1985) p. 11.

[12] E. D. Palik, in *Handbook of Optical Constants of Solids II*, edited by E. D. Palik (Academic Press Inc., San Diego, 1991) p. 8.

[13] H. A. MacLeod, *Thin Film Optical Filters* (Adam Hilger, Bristol, 1986).

[14] B. Harbecke, Appl. Phys. B **39**, 165 (1986).

[15] L. Vriens and M. Rippens, Appl. Opt. **22**, 4105 (1983).

[16] A. H. M. Holtslag and P. M. L. O. Scholte, Appl. Opt. **28**, 5095 (1989).

[17] H. R. Philipp, in *Handbook of Optical Constants of Solids I*, edited by E. D. Palik (Academic Press Inc., San Diego, 1985) p. 749.

[18] Shiga T, Fujikawa H and Taga Y 2003 Design of multiwavelength resonant cavities for white organic light emitting diodes *J. Appl. Phys.* **93** 19-22

[19] Bulović V, Khalfin V B, Gu G, Burrows P, Garbuzov D Z and Forrest S R 1998 Weak microcavity effects in organic light-emitting devices *Phys. Rev. B* **58** 3730-3740

[20] Dodabalapur A, Rothberg L J, Jordan R H, Miller T M, Slusher R E and Phillips J M 1996 Physics and applications of organic microcavity light emitting diodes J. Appl. Phys. 80 6954-6964

[21] C. Tang, S. VanSlyke and C. Chen, "Electroluminescence of Doped Organic Thin Films", J. Appl. Phys. 85, pp.3610, 1989.

[22] Y. Yamamoto, S. Machida, K. Igeta and G. Bjork, "Controlled Spontaneous Emission in Microcavity Semiconductor Lasers" in Y. Yamamoto Ed. "Coherence, Amplification and Quantum Effects in Semiconductor Lasers", J. Wiley and Sons, Inc. New York, 1991.